Scientific paper

Synthesis, Crystal Structures and Urease Inhibition of Mononuclear Copper(II) and Nickel(II) Complexes with Schiff Base Ligands

Jian Jiang,[1,*] Peng Liang,[2] Huiyuan Yu[3] and Zhonglu You[3]

[1] *College of Chemical Engineering and Machinery, Eastern Liaoning University, Dandong 118003, P. R. China*

[2] *School of Engineering and Technology, Eastern Liaoning University, Dandong 118003, P. R. China*

[3] *Department of Chemistry and Chemical Engineering, Liaoning Normal University, Dalian 116029, P. R. China*

* *Corresponding author: E-mail: jiangjiandd2012@126.com*

Received: 03-30-2022

Abstract

Three mononuclear copper(II) and nickel(II) complexes, [Cu(L^1)(NCS)(CH_3OH)] (**1**), [Cu(L^2)(NCS)] (**2**) and [Ni(L^2)(N_3)] (**3**), where L^1 and L^2 are the monoanionic forms of the Schiff bases *N*'-(pyridin-2-ylmethylene)picolinohydrazide (HL^1) and 4-methyl-2-(((pyridin-2-ylmethyl)imino)methyl)phenol (HL^2), have been prepared and characterized by elemental analysis, IR and UV-Vis spectroscopy, as well as single crystal X-ray diffraction studies. The Cu atom in complex **1** is in a square pyramidal coordination, with the three N atoms of the ligand L and the N atom of the thiocyanate ligand in the basal plane, and with the methanol O atom at the apical position. The Cu and Ni atoms in complexes **2** and **3** are in square planar coordination, with the three donor atoms of the Schiff base ligands and the terminal N atoms of thiocyanate and azide ligands. Complexes **1** and **2** inhibit the *Jack bean* urease with IC_{50} value of 0.33 ± 0.12 and 0.39 ± 0.10 μmol L^{-1}, respectively. Molecular docking study was performed to investigate the interaction between the complexes and the enzyme.

Keywords: Schiff base; Copper complex; Nickel complex; Crystal structure; Urease inhibition

1. Introduction

Urease is a nickel-containing enzyme, which widely be found in bacteria, fungi, algae, plants, and even in soil. The enzyme catalyzes the hydrolysis of urea to produce NH_3 with the rate 10^{14} times faster than that without urease. This process leads to a significant increase in pH of soil, and damage the plants.[1] In human being and animals, urease plays a vital role in peptic ulceration, urinary catheter incrustation, kidney stone, pyelonephritis, urolithiasis, hepatic encephalopathy and arthritis.[2] Thus, the control of side effects of the urease is a hot topic in science. Urease inhibitors have been proved to be the best way to control the activity of urease. A variety of urease inhibitors have been reported, including inorganic metal salts,[3] hydroxamic acid derivatives, triazoles, semicarbazones, Schiff bases, urea derivatives, oxadiazole, *etc.*[4] However, most of them were prevented from application because of their low inhibition efficiency.[5] Inorganic urease inhibitors such as the nitrate and chloride salts of copper, have effective activities. However, they are harmful to both soil and living organisms.[6] Recent reports indicated that some Schiff base copper(II) complexes have good urease inhibitory activities.[7] Khan and co-workers reported that some hydrazones have potential urease inhibitory activity. The diacyl hydrazide group (–NH–N=CH–) in the compounds serves as stabilizing agent in the active site and prevent the binding of substrate. In addition to stabilize the inhibitors, the –NH group of diacyl hydrazide was involved making strong hydrogen bonds with amino acid Arg439 and Ala636 of the urease.[8] Considering that copper and nickel complexes with Schiff bases have a wide range of biological applications,[9] in the present work, three mononuclear copper(II) and nickel(II) complexes, [Cu(L^1)(NCS)(CH_3OH)] (**1**), [Cu(L^2)(NCS)] (**2**) and [Ni(L^2)(N_3)] (**3**), where L^1 and L^2 are the monoanionic forms of the Schiff bases *N*'-(pyridin-2-ylmethylene)picolinohydrazide (HL^1, Scheme 1) and 4-methyl-2-(((pyridin-2-ylmethyl)imino)methyl) phenol (HL^2, Scheme 1) are presented.

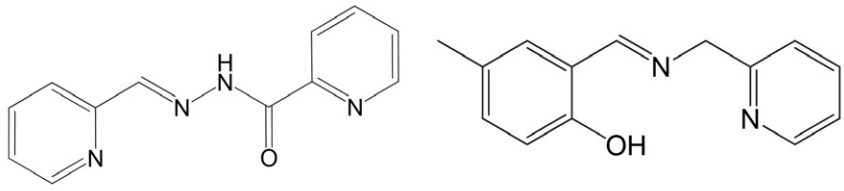

HL[1] HL[2]

Scheme 1. The Schiff base ligands.

2. Experimental

2. 1. Materials and Measurements

2-Pyridinecarboxaldehyde, 2-picolinyl hydrazide, 5-methylsalicylaldehyde, 2-aminomethylpyridine, copper acetate, copper nitrate, nickel nitrate, ammonium thiocyanate, sodium azide and solvents with AR grade were purchased from Xiya Chemicals Co. Ltd. (China). Elemental analyses for C, H and N were performed on a Perkin-Elmer 240C elemental analyzer. IR spectra were recorded on a Jasco FT/IR-4000 spectrometer as KBr pellets in the 4000–400 cm^{-1} region. Electronic spectra were recorded on a Lambda 35 spectrophotometer. ^1H and ^{13}C NMR were recorded on a Bruker 300 MHz instrument. Single crystal X-ray diffraction was carried out on a Bruker SMART 1000 CCD diffractometer.

2. 2. Synthesis of *N*'-(Pyridin-2-ylmethylene) picolinohydrazide (HL^1)

2-Pyridinecarboxaldehyde (1.1 g, 0.010 mol) and 2-picolinyl hydrazide (1.4 g, 0.010 mol) were mixed in methanol (50 mL). The mixture was stirred at 25 °C for 30 min to give colorless solution. Then the solvent was evaporated to give gummy product, which was re-crystallized from ethanol to give yellow crystalline product of HL^1. Yield: 1.8 g (80%). M.p. 172–173 °C. Anal. Calc. for $C_{12}H_{10}N_4O$ (%): C, 63.71; H, 4.46; N, 24.76. Found (%): C, 63.53; H, 4.60; N, 24.63. IR data (cm^{-1}): 3290w (NH), 1698s (C=O), 1647m (C=N). ^1H NMR (300 MHz, $CDCl_3$): δ 11.18 (s, 1H, N*H*), 8.89 (d, 1H, Py*H*), 8.72 (d, 1H, Py*H*), 8.35 (d, 1H, Py*H*), 7.90 (t, 1H, Py*H*), 7.88 (d, 1H, Py*H*), 7.81 (m, 2H, Py*H*), 7.62 (m, 1H, Py*H*), 7.28 (s, 1H, C*H*=N). ^{13}C NMR (75 MHz, $CDCl_3$): δ 159.79, 152.14, 151.80, 149.56, 148.31, 147.70, 137.14, 136.56, 126.46, 125.98, 122.54, 121.02.

2. 3. Synthesis of 4-Methyl-2-(((pyridin-2-ylmethyl)imino)methyl)phenol (HL^2)

2-Pyridinecarboxaldehyde (1.1 g, 0.010 mol) and 2-aminomethylpyridine (1.1 g, 0.010 mol) were mixed in methanol (50 mL). The mixture was stirred at 25 °C for 30 min to give colorless solution. Then the solvent was evaporated to give gummy product, which was re-crystallized from ethanol to give yellow crystalline product of HL^2. Yield: 1.9 g (84%). M.p. 155–156 °C. Anal. Calc. for $C_{14}H_{14}N_2O$ (%): C, 74.31; H, 6.24; N, 12.38. Found (%): C, 74.45; H, 6.32; N, 12.23. IR data (cm^{-1}): 3378w (OH), 1638m (C=N). ^1H NMR (300 MHz, $CDCl_3$): δ 10.32 (s, 1H, O*H*), 8.72 (s, 1H, C*H*=N), 8.43 (d, 1H, Py*H*), 7.71 (t, 1H, Py*H*), 7.52 (s, 1H, Py*H*), 7.27 (t, 1H, Py*H*), 7.15–7.10 (m, 2H, Py*H*), 6.83 (d, 1H, Py*H*), 5.21 (s, 2H, CH_2), 2.32 (s, 3H, CH_2). ^{13}C NMR (75 MHz, $CDCl_3$): δ 161.23, 159.31, 158.27, 148.46, 137.87, 133.53, 132.02, 130.55, 123.72, 121.55, 120.63, 115.91, 64.83, 21.72.

2. 4. Synthesis of Methanol-isothiocyanato-(*N*'-(pyridin-2-ylmethylene) picolinohydrazido)copper(II) (1)

HL^1 (0.023 g, 0.10 mmol), copper nitrate trihydrate (0.024 g, 0.10 mmol) and ammonium thiocyanate (0.0076 g, 0.10 mmol) were mixed in methanol (30 mL). The mixture was stirred at ambient temperature for 30 min to give blue solution. The solvent was slowly evaporated to give single crystals. Yield: 0.013 g (34%). Anal. Calc. for $C_{14}H_{13}CuN_5O_2S$ (%): C, 44.38; H, 3.46; N, 18.48. Found (%): C, 44.53; H, 3.55; N, 18.37. IR data (cm^{-1}): 3438w (OH), 2081s (NCS), 1645s (C=O), 1598s (C=N), 1560s, 1475w, 1386m, 1332w, 1289w, 1251w, 1167m, 1082m, 1040m, 760w, 688w, 579w, 511w, 472w. UV–Vis data (methanol, λ/nm (ε/M^{-1} cm^{-1})): 215 (17,565), 255 (11,450), 367 (13,270).

2. 5. Synthesis of Isothiocyanato-(4-methyl-2-(((pyridin-2-ylmethyl)imino)methyl) phenolato)copper(II) (2)

Complex **2** was prepared by following the same method as described in section 2.4 for complex **1**, but with HL^1 replaced by HL^2 (0.023 g, 0.10 mmol). Yield: 0.016 g (46%). Anal. Calc. for $C_{15}H_{13}CuN_3OS$ (%): C, 51.94; H, 3.78; N, 12.11. Found (%): C, 51.77; H, 3.86; N, 11.98. IR data (cm^{-1}): 2078s (NCS), 1629s (C=N), 1528w, 1461m, 1417w, 1385m, 1318w, 1276w, 1215m, 1160m, 1121w, 1071w, 1052m, 842m, 802w, 761m, 709w, 608w, 561w, 525w, 475w. UV–Vis data (methanol, λ/nm (ε/M^{-1} cm^{-1})): 223 (19,675), 246 (17,630), 272 (15,352), 385 (4,533).

2. 6. Synthesis of Azido-(4-methyl-2-(((pyridin-2-ylmethyl)imino)methyl) phenolato)nickel(II) (3)

Complex **3** was prepared by the same method as described for complex **2**, but with ammonium thiocyanate replaced by sodium azide (0.0065 g, 0.10 mmol), and with copper nitrate trihydrate replaced by nickel nitrate hexahydrate (0.029 g, 0.10 mmol). Yield: 0.019 g (58%). Anal. Calc. for $C_{14}H_{13}N_5NiO$ (%): C, 51.58; H, 4.02; N, 21.48. Found (%): C, 51.39; H, 3.92; N, 21.37. IR data (cm^{-1}): 2041s (N_3), 1627s (C=N), 1530w, 1471m, 1449w, 1387m, 1318w, 1279w, 1222m, 1168m, 1140w, 1118w, 1074m, 1054m, 983w, 822m, 763m, 709w, 610w, 560w, 533w, 464w. UV–Vis data (methanol, λ/nm (ε/M^{-1} cm^{-1})): 223 (18,720), 242 (17,315), 283 (8,120), 383 (6,350).

2. 7. X-ray Diffraction

Diffraction intensities for the complexes were collected at 298(2) K using a Bruker SMART 1000 CCD area-detector diffractometer with MoKα radiation (λ = 0.71073 Å). The collected data were reduced with the SAINT,[10] and multi-scan absorption correction was performed using the SADABS.[11] The structures were solved by direct method and refined against F^2 by full-matrix least-squares method using the SHELXL package.[12] All of the non-hydrogen atoms were refined anisotropically. Hydrogen atoms were placed in calculated positions and constrained to ride on their parent atoms. The crystallographic data for the complexes are summarized in Table 1.

2. 8. Urease Inhibitory Activity Assay

The measurement of urease inhibitory activity was carried out according to the literature method.[13] The assay mixture containing 75 μL of *Jack bean* urease and 75 μL of tested compounds with various concentrations (dissolved in DMSO) was preincubated for 15 min on a 96-well assay plate. Acetohydroxamic acid was used as a reference. Then 75 μL of phosphate buffer at pH 6.8 containing phenol red (0.18 mmol L^{-1}) and urea (400 mmol L^{-1}) were added and incubated at 25 °C. The reaction time required for enough ammonium carbonate to form to raise the pH of the phosphate buffer from 6.8 to 7.7 was measured by a micro-plate reader (560 nm) with the end-point being determined by the color change of phenol-red indicator.

2. 6. Molecular Docking Study

Molecular docking study of the molecules of complexes **1** and **2** into the 3D X-ray structure of the *Jack bean* urease was carried out by using the AutoDock 4.0 software as implemented through the graphical user interface Au-

Table 1. Crystal data for the complexes

	1	**2**	**3**
Chemical Formula	$C_{14}H_{13}CuN_5O_2S$	$C_{15}H_{13}CuN_3OS$	$C_{14}H_{13}N_5NiO$
Fw	378.89	346.88	326.00
T (K)	298(2)	298(2)	298(2)
λ (Mo K*α*) (Å)	0.71073	0.71073	0.71073
Crystal system	Triclinic	Monoclinic	Triclinic
Space group	*P*–1	$P2_1/n$	*P*–1
a (Å)	7.0645(10)	6.9831(12)	7.3030(11)
b (Å)	10.6425(14)	15.342(1)	9.0155(10)
c (Å)	11.4005(16)	13.333(1)	10.5740(12)
a (°)	69.749(2)	90	88.622(1)
b (°)	75.837(2)	91.873(1)	77.044(1)
g (°)	85.187(2)	90	85.605(1)
V (Å^3)	779.71(19)	1427.7(3)	676.5(2)
Z	2	4	2
m (Mo K*α*) (cm^{-1})	1.550	1.677	1.601
D_c (g cm^{-3})	1.614	1.614	1.601
Reflections	4179	8002	3662
Unique reflections	2885	2639	2307
Observed reflections [$I \geq 2s(I)$]	2354	1418	1939
Parameters	212	191	191
Restraints	3	0	0
Goodness of fit on F^2	1.030	0.984	1.054
R_{int}	0.0166	0.1392	0.0195
R_1 [$I \geq 2s(I)$]	0.0474	0.0767	0.0347
wR_2 [$I \geq 2s(I)$]	0.1106	0.1278	0.0765
R_1 (all data)	0.0625	0.1538	0.0461
wR_2 (all data)	0.1194	0.1490	0.0820
$\Delta\rho_{max}/\Delta\rho_{min}$, *e* Å^{-3}	1.074/–0.320	0.437/–0.380	0.393/–0.288

toDockTools (ADT 1.5.2). In the docking, grid box size of 40 × 50 × 58 Å^3 for the complex points in *x*, *y*, and *z* directions was built, the maps were centered on the original ligand molecule in the catalytic site of the protein. A grid spacing of 0.375 Å and a distance-dependent function of the dielectric constant were used for the calculation of the energetic map. 100 runs were generated by using Lamarckian genetic algorithm searches. Default settings were used with an initial population of 50 randomly placed individuals, a maximum number of 2.5 × 10^6 energy evaluations, and a maximum number of 2.7 × 10^4 generations. A mutation rate of 0.02 and a crossover rate of 0.8 were chosen. The results of the most favorable free energy of binding were selected as the resultant complex structures.

3. Results and Discussion

3. 1. Chemistry

The Schiff bases HL^1 and HL^2 were readily prepared by the condensation reaction of equimolar quantities of 2-pyridinecarboxaldehyde with 2-picolinyl hydrazide, and 5-methylsalicylaldehyde with 2-aminomethylpyridine, respectively, in methanol. The copper complexes **1** and **2** were prepared by the reaction of equimolar quantities of the Schiff bases, copper nitrate and ammonium thiocyanate in methanol. To study the influence of the anions of copper salts on the structures of the complexes, we tried to use copper acetate in the syntheses, yet, the same structures as those prepared with copper nitrate have been obtained. The nickel complex **3** was prepared by the reaction of equimolar quantities of the Schiff base, nickel nitrate and sodium azide in methanol. The complexes are soluble in methanol, ethanol, acetonitrile, DMSO and DMF. Single crystals were obtained by slow evaporation of the methanolic solution of the complexes. The free Schiff bases and the complexes are stable in air at 25 °C.

3. 2. Structure Description of Complex 1

The molecular structure of the complex is shown in Fig. 1. Selected bond lengths and angles are given in Table 2. The Cu atom is five-coordinated in a square pyramidal geometry, with the three nitrogen atoms (N1, N3, N4) of the Schiff base ligand L and the thiocyanate nitrogen atom (N5) defining the basal plane, and with the methanol oxygen atom (O2) occupying the apical position. The distortion of the square pyramidal coordination can be observed by the bond angles around the Cu center. The *cis* and *trans* angles in the basal plane are 82.31(14)–94.32(15)° and 168.66(13)–174.99(16)°, respectively. The bond angles among the apical and basal donor atoms are 89.22(14)–96.05(11)°. The Cu–N bond lengths related to the Schiff base ligand are 1.938(3)–2.033(3) Å, and the Cu–N bond length related to the thiocyanate ligand is 1.964(4) Å, which are comparable to the copper(II) complexes with similar ligands.[14] The apical bond length of Cu1–O2 is

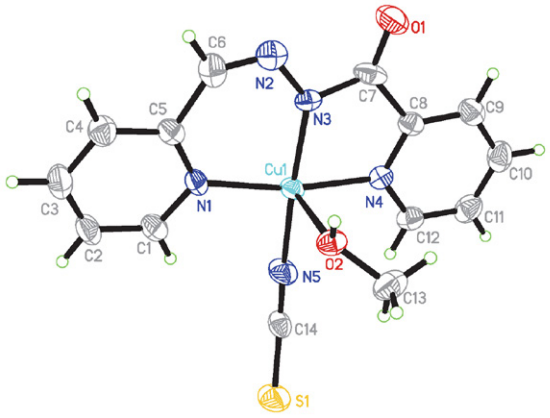

Fig. 1. A perspective view of the molecular structure of complex **1** with the atom labeling scheme. Thermal ellipsoids are drawn at the 30% probability level.

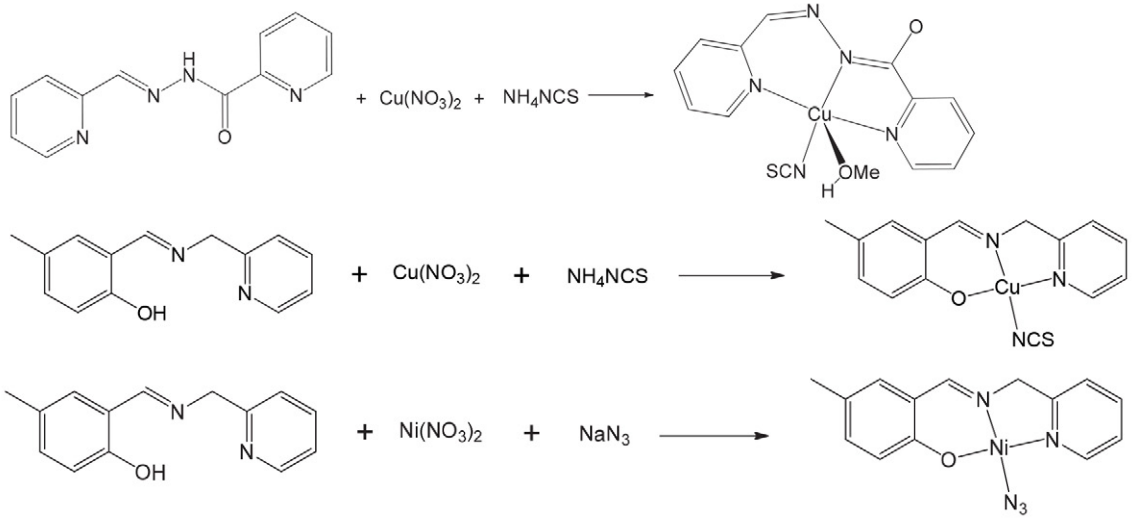

Scheme 3. The synthetic procedure for the complexes.

longer than the basal bonds, which is not uncommon for methanol coordinated complexes.[15]

In the crystal structure of the complex, two adjacent molecules are linked through intermolecular O–H···N and O–H···O hydrogen bonds (Table 3), to form a dimer. The dimers are linked through intermolecular C–H···O hydrogen bonds (Table 3), to form ladder like chains along the *b* axis (Fig. 2). Moreover, there are $\pi\cdots\pi$ interactions among the molecules (Table 4).

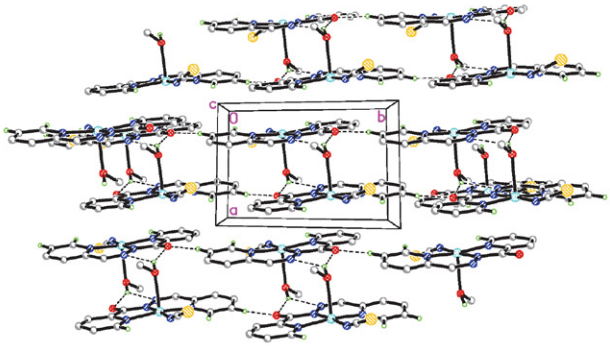

Fig. 2. Molecular packing diagram of complex **1**, viewed along the *c* axis. Hydrogen bonds are shown as dashed lines.

Table 2. Selected bond lengths (Å) and angles (°) for the complexes

		1	
Cu1–N1	2.033(3)	Cu1–N3	1.938(3)
Cu1–N4	2.033(3)	Cu1–N5	1.964(4)
Cu1–O2	2.365(3)		
N3–Cu1–N5	174.99(16)	N3–Cu1–N1	90.05(14)
N5–Cu1–N1	94.32(15)	N3–Cu1–N4	82.31(14)
N5–Cu1–N4	93.00(15)	N1–Cu1–N4	168.66(13)
N3–Cu1–O2	92.76(12)	N5–Cu1–O2	89.22(14)
N1–Cu1–O2	96.05(11)	N4–Cu1–O2	92.69(12)
		2	
Cu1–O1	1.895(4)	Cu1–N1	2.004(5)
Cu1–N2	1.921(5)	Cu1–N3	1.936(6)
O1–Cu1–N2	93.73(19)	O1–Cu1–N3	89.7(2)
N2–Cu1–N3	176.4(2)	O1–Cu1–N1	176.10(19)
N2–Cu1–N1	82.4(2)	N3–Cu1–N1	94.2(2)
		3	
Ni1–O1	1.831(2)	Ni1–N1	1.842(2)
Ni1–N2	1.908(2)	Ni1–N3	1.909(3)
O1–Ni1–N1	94.84(10)	O1–Ni1–N2	178.74(9)
N1–Ni1–N2	84.92(10)	O1–Ni1–N3	88.10(11)
N1–Ni1–N3	176.74(11)	N2–Ni1–N3	92.18(12)

3. 3. Structure Description of Complexes 2 and 3

The molecular structures of complexes **2** and **3** are shown in Figs. 3 and 4, respectively. Selected bond lengths and angles are given in Table 2. Both the complexes are of distorted square planar geometry. The Cu and Ni atoms are coordinated by the phenolate O, imino N and pyridine N atoms of the Schiff base ligands, and the N atoms of thiocyanate (for **2**) and azide (for **3**) ligands. The distortion of the square planar coordination can be observed by the bond angles around the metal centers. The *cis* and *trans* angles are 82.4(2)–94.2(2)° and 176.1(2)–176.4(2)° for **2**, and 84.9(1)–94.8(1)° and 176.7(1)–178.7(1)° for **3**, respectively. The Cu–O and Cu–N bond lengths in complex **2** are longer than the Ni–O and Ni–N bond lengths in complex **3**, which are in accordance with the bond values observed in similar copper(II) and nickel(II) complexes with Schiff base ligands.[14,16]

In the crystal structure of complex **2**, the molecules are stacked with $\pi\cdots\pi$ interactions (Table 4, Fig. 5). In the crystal structure of complex **3**, two adjacent molecules are linked through intermolecular C–H···N hydrogen bonds (Table 3), to form a dimer (Fig. 6). Moreover, there are $\pi\cdots\pi$ interactions among the molecules (Table 4).

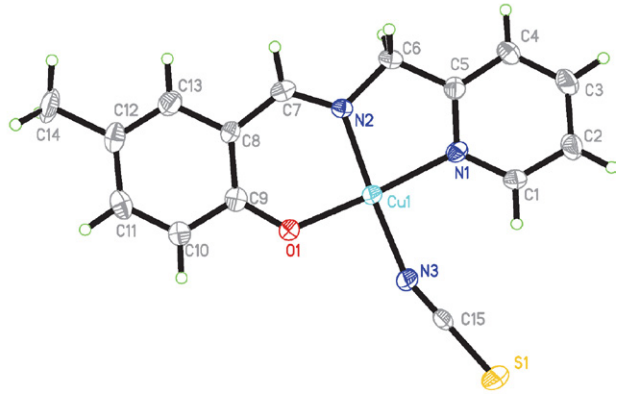

Fig. 3. A perspective view of the molecular structure of complex **2** with the atom labeling scheme. Thermal ellipsoids are drawn at the 30% probability level.

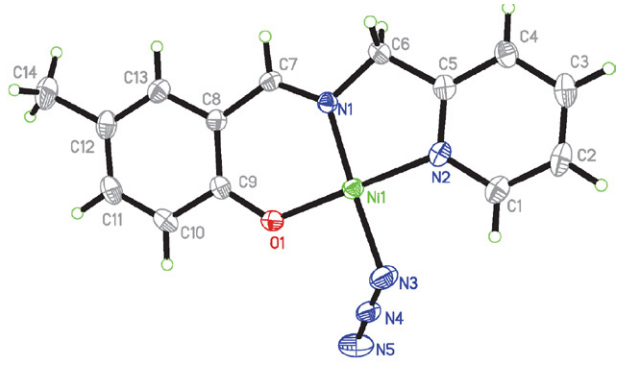

Fig. 4. A perspective view of the molecular structure of complex **3** with the atom labeling scheme. Thermal ellipsoids are drawn at the 30% probability level.

3. 4. IR Spectra

The infrared spectra of the free Schiff bases and the complexes were recorded in the region of 4000–400

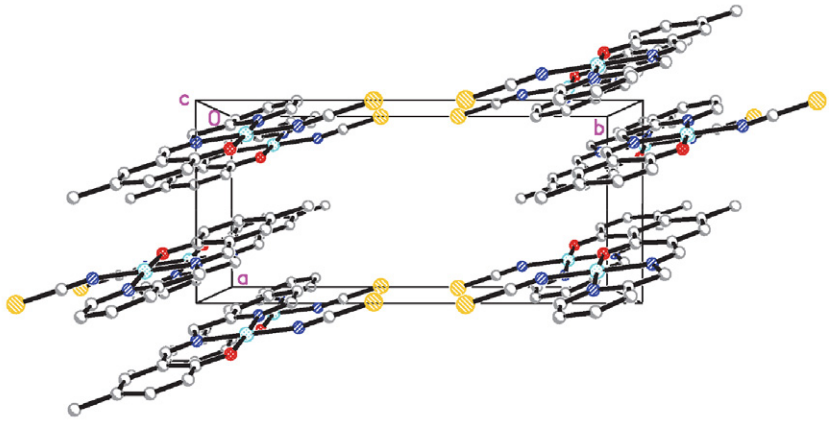

Fig. 5. Molecular packing diagram of complex **2**, viewed along the *c* axis.

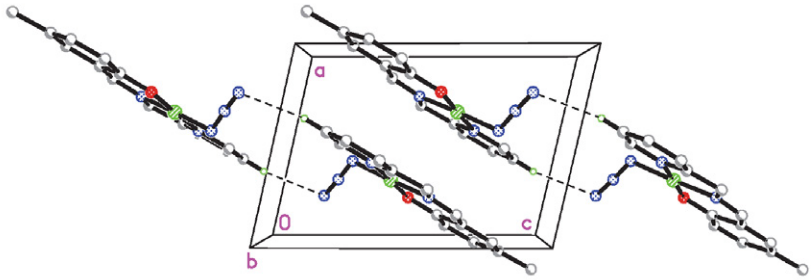

Fig. 6. Molecular packing diagram of complex **3**, viewed along the *b* axis. Hydrogen bonds are shown as dashed lines.

Table 3. Hydrogen bond distances (Å) and bond angles (°) for complexes **1** and **3**

D–H···*A*	*d*(*D*–H)	*d*(H···*A*)	*d*(*D*···*A*)	Angle (*D*–H···*A*)
		1		
O2–H2···N2^{i}	0.86(1)	2.40(3)	3.038(5)	132(3)
O2–H2···O1^{i}	0.86(1)	2.09(2)	2.852(5)	148(3)
C2–H2A···O1	0.93	2.48(2)	3.399(5)	170(3)
		3		
C2–H2···N5^{ii}	0.93	2.62(3)	3.510(5)	161(4)

Symmetry codes: (i) 1 – *x*, 1 – *y*, 1 – *z*; (ii) 1 – *x*, 1 – *y*, – *z*.

Table 4. π···π interactions of the complexes

Cg···*Cg*	distance (Å)	*Cg*···*Cg*	distance (Å)
1			
*Cg*1···*Cg*1^{iii}	3.448(5)	*Cg*1···*Cg*2^{iii}	3.818(5)
*Cg*1···*Cg*2^{i}	4.445(5)	*Cg*1···*Cg*3^{iii}	4.645(5)
*Cg*2···*Cg*2^{i}	4.938(5)	*Cg*2···*Cg*3^{iii}	3.636(5)
*Cg*4···*Cg*4^{i}	3.935(5)	*Cg*4···*Cg*3^{iii}	4.651(5)
2			
*Cg*5···*Cg*6^{i}	3.794(4)	*Cg*1···*Cg*2^{iv}	4.967(4)
*Cg*5···*Cg*8^{i}	3.507(4)	*Cg*1···*Cg*4^{iv}	3.569(4)
*Cg*6···*Cg*6^{i}	3.389(4)	*Cg*2···*Cg*2^{iv}	3.612(4)
*Cg*6···*Cg*8^{i}	4.610(4)	*Cg*2···*Cg*4^{iv}	3.601(4)
*Cg*7···*Cg*8^{i}	3.721(4)	*Cg*3···*Cg*4^{iv}	4.823(4)
3			
*Cg*9···*Cg*9^{i}	3.982(4)	*Cg*1···*Cg*2^{iii}	4.006(4)
*Cg*9···*Cg*10^{i}	3.558(4)	*Cg*1···*Cg*4^{iii}	3.563(4)
*Cg*9···*Cg*12^{i}	4.776(4)	*Cg*2···*Cg*2^{iii}	3.479(4)
*Cg*10···*Cg*10^{i}	4.624(4)	*Cg*2···*Cg*3^{i}	3.781(4)
*Cg*10···*Cg*12^{iii}	4.530(4)	*Cg*3···*Cg*4^{iii}	3.799(4)
*Cg*11···*Cg*12^{i}	3.638(4)		

Symmetry codes: iii: – *x*, 1 – *y*, 1 – *z*; iv: 2 – *x*, 1 – *y*, 1 – *z*. *Cg*1, *Cg*2, *Cg*3 and *Cg*4 are the centroids of Cu1-N3-C7-C8-N4, Cu1-N1-C5-C6-N2-N3, N4-C8-C9-C10-C11-C12 and N1-C1-C2-C3-C4-C5 in complex **1**, respectively. *Cg*5, *Cg*6, *Cg*7 and *Cg*8 are the centroids of Cu1-N1-C5-C6-N2, Cu1-O1-C9-C8-C7-N2, N1-C1-C2-C3-C4-C5 and C8-C9-C10-C11-C12-C13 in complex **2**, respectively. *Cg*9, *Cg*10, *Cg*11 and *Cg*12 are the centroids of Ni1-N1-C6-C5-N2, Ni1-O1-C9-C8-C7-N1, N2-C1-C2-C3-C4-C5 and C8-C9-C10-C11-C12-C13 in complex **3**, respectively.

cm^{-1} using KBr pellets. There is a weak and sharp band at 3290 cm^{-1} in the spectrum of HL^{1}, which is assigned to the NH vibration. The broad and weak bands at 3378-3438 cm^{-1} of HL^{2} and complex **1** can be assigned to the OH vibrations. The bands at 1647 cm^{-1} for HL^{1} and 1645 cm^{-1} for complex **1** are due to the azomethine group, μ(C=N).[17] They are almost in the same frequency, indicates that the imine N atom is not participate in coordination. The intense band for the C=O group is observed at 1698 cm^{-1} for HL^{1}. The absence of the band in the spectrum of complex **1** indicates that the C=O group turned to other form. The bands at 1638 cm^{-1} for HL^{2} and 1627–1629 cm^{-1} for complexes **2** and **3** are due to the azomethine group.[17] The shift to lower frequencies

in the spectra of the complexes indicates that the imine N atoms form coordination bonds with the metal atoms. The typical absorption for the thiocyanate ligands in complexes **1** and **2** is observed at 2078–2081 cm^{-1}.[18] The typical absorption for the azide ligand in complex **3** is observed at 2041 cm^{-1}.[19]

3. 5. Urease Inhibitory Activity

Complexes **1** and **2** have excellent inhibitory activity on the *Jack bean* urease, with IC_{50} values of 0.33 ± 0.27 and 0.39 ± 0.10 μmol L^{-1}, respectively, whereas the free Schiff bases HL^1 and HL^2, and the nickel complex **3** have weak activity (> 50 μmol L^{-1}). The reported copper complexes have shown better activity than the reference drug acetohydroxamic acid (IC_{50} = 28.5 ± 2.7 μmol L^{-1}) and the copper nitrate (IC_{50} = 8.6 ± 1.5 μmol L^{-1}). The two copper complexes have better activity against urease than the copper(II) complex with the Schiff base ligand *N,N*'-bis(4-fluorosalicylidene)-1,2-diaminopropane (IC_{50} = 2.1–3.4 μmol L^{-1}),[20] and the copper(II) complex with the reduced Schiff base ligand 2,2'-((propane-1,3-diylbis(azanediyl))bis(methylene)diphenol (IC_{50} = 1.6 μmol L^{-1}).[21]

3. 6. Molecular Docking Study on Complexes 1 and 2

Molecular docking study was performed to inspect the binding effects between the molecules of complexes **1** and **2** with the *Jack bean* urease. The binding models of the complexes with the urease are depicted in Figs. 7 and 8. The results indicate that the complex molecules fit well with the active site of the urease. The interactions of the complex molecules with the urease have been established in a variety of conformations because of the flexibility of the molecules and the amino acid residues of the urease. The binding energy is –5.78 kcal/mol for **1** and –5.78 kcal/mol for **2**. It is lower than the binding energy of the AHA inhibited model (–5.01 kcal/mol). The negative values reveal that the complex molecules combine well with the center of the urease.

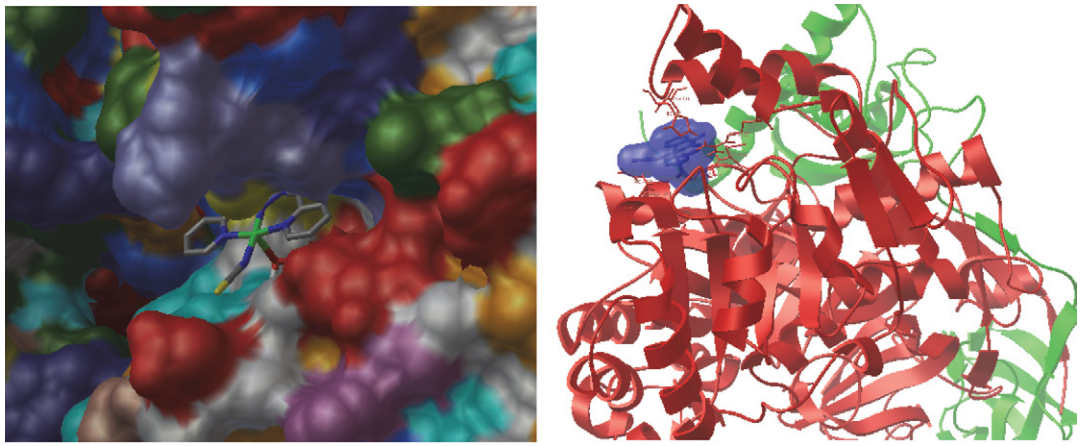

Fig. 7. Binding mode of the molecule of complex **1** with *Jack bean* urease. Left: The enzyme is shown as surface, and the complex is shown as sticks. Right: The enzyme is shown as ribbons, and the complex is shown as a filling model.

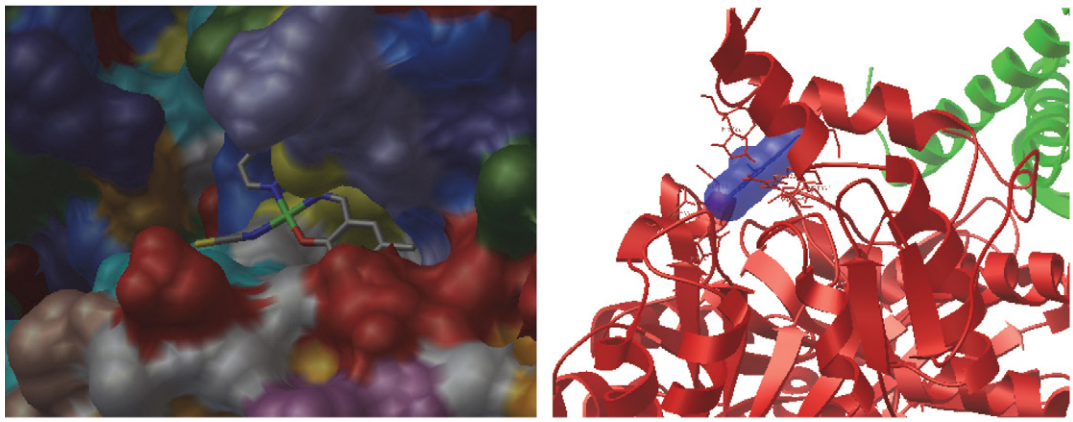

Fig. 8. Binding mode of the molecule of complex **2** with *Jack bean* urease. Left: The enzyme is shown as surface, and the complex is shown as sticks. Right: The enzyme is shown as ribbons, and the complex is shown as a filling model.

4. Conclusion

In summary, the present paper intends to report the syntheses, crystal structures and urease inhibition activity of three mononuclear copper(II) and nickel(II) complexes with the tridentate Schiff base ligands *N*'-(pyridin-2-ylmethylene)picolinohydrazide and 4-methyl-2-(((pyridin-2-ylmethyl)imino)methyl)phenol. Both the copper complexes have shown effective inhibitory activity on *Jack bean* urease.

Appendix A. Supplementary material

CCDC 2160252 (**1**), 2163190 (**2**) and 2163191 (**3**) contain the supplementary crystallographic data for this article. These data can be obtained free of charge at http://www.ccdc.cam.ac.uk/const/retrieving.html or from the Cambridge Crystallographic Data Centre (CCDC), 12 Union Road, Cambridge CB2 1EZ, UK; Fax: +44(0)1223-336033 or E-mail: deposit@ccdc.cam.ac.uk.

5. References

1. (a) A. Ray, C. Nkwonta, P. Forrestal, M. Danaher, K. Richards, T. O'Callaghan, S. Hogan, E. Cummins, *Rev. Environ. Health* **2021**, *36*, 477–491; **DOI:**10.1515/reveh-2020-0088
   (b) T. Lan, Y. X. Huang, X. Song, O. P. Deng, W. Zhou, L. Luo, X. Y. Tang, J. Zeng, G.D. Chen, X. S. Gao, *Environ. Pollut.* **2021**, *293*, 118499; **DOI:**10.1016/j.envpol.2021.118499
   (c) M. P. Byrne, J. T. Tobin, P. J. Forrestal, M. Danaher, C. G. Nkwonta, K. Richards, E. Cummins, S.A. Hogan, T. F. O'Callaghan, *Sustainability* **2020**, *12*, 6018. **DOI:**10.3390/su12156018
2. (a) A.T. Fiori-Duarte, R.P. Rodrigues, R.R. Kitagawa, D.F. Kawano, *Curr. Med. Chem.* **2020**, *27*, 3967–3982; **DOI:**10.2174/0929867326666190301143549
   (b) M. Taha, N. H. Ismail, S. Imran, A. Wadood, F. Rahim, M. Riaz, *J. Bioorg. Med. Chem.* **2015**, *23*, 7211–7218. **DOI:**10.1016/j.bmc.2015.10.017
3. (a) G. I. Perez-Perez, C. B. Gower, M. J. Blaser, *Infect. Immun.* **1994**, *62*, 299–302. **DOI:**10.1128/iai.62.1.299-302.1994
4. (a) R. Mamidala, S. R. S. Bhimathati, A. Vemn, *Bioorg. Chem.* **2021**, *114*, 105010; **DOI:**10.1016/j.bioorg.2021.105010
   (b) S. Iqbal, A. Khan, R. Nazir, S. Kiran, S. Perveen, K. M. Khan, M.I. Choudhary, *Med. Chem.* **2020**, *16*, 244–255; **DOI:**10.2174/1573406415666190415163309
   (c) S. Daud, O.U.R. Abid, A. Sardar, B.A. Shah, M. Rafiq, A. Wadood, M. Ghufran, W. Rehman, Zain-ul-Wahab, F. Iftikhar, R. Sultana, H. Daud, B. Niaz, *Med. Chem. Res.* **2022**, *31*, 316–336; **DOI:**10.1007/s00044-021-02814-6
   (d) M. Talebi, E. Hamidian, F. Niasari-Naslaji, S. Rahmani, F. S. Hosseini, S. Boumi, M. N. Montazer, M. Asadi, M. Amanlou, *Med. Chem. Res.* **2021**, *30*, 1220–1229; **DOI:**10.1007/s00044-021-02727-4
   (e) M. A. S. Aslam, S. Mahmood, M. Shahid, A. Saeed, J. Iqbal, *Eur. J. Med. Chem.* **2011**, *46*, 5473–5479; **DOI:**10.1016/j.ejmech.2011.09.009
   (f) E. Menteşe, M. Emirik, B.B. Sökmen, *Bioorg. Chem.* **2019**, *86*, 151–158. **DOI:**10.1016/j.bioorg.2019.01.061
5. (a) Z.-J. Chen, Y.-N. Chen, C.-N. Xu, S.-S. Zhao, Q.-Y. Cao, S.-S. Qian, J. Qin, H.-L. Zhu, *J. Mol. Struct.* **2016**, *1117*, 293–299; **DOI:**10.1016/j.molstruc.2016.03.084
   (b) Z.-P. Xiao, Z.-Y. Peng, J.-J. Dong, R.-C. Deng, X.-D. Wang, H. Ouyang, P. Yang, J. He, Y.-F. Wang, M. Zhu, X.-C. Peng, W.-X. Peng, H.-L. Zhu, *Eur. J. Med. Chem.* **2013**, *68*, 212–221.
6. (a) B. Krajewska, *J. Mol. Catal. B: Enzym.* **2009**, *59*, 9–21; **DOI:**10.1016/j.molcatb.2009.01.003
   (b) L. Habala, F. Devínsky, A.E. Egger, *J. Coord. Chem.* **2018**, *71*, 907–940. **DOI:**10.1080/00958972.2018.1458228
7. (a) H. Pervez, M. Ahmad, S. Zaib, M. Yaqub, M. M. Naseer, J. Iqbal, *MedChemComm* **2016**, *7*, 914–923; **DOI:**10.1039/C5MD00529A
   (b) H. Pervez, N. Khan, J. Iqbal, S. Zaib, M. Yaqub, M. M. Naseer, *Acta Chim. Slov.* **2018**, *65*, 108–118; **DOI:**10.17344/acsi.2017.3649
   (c) H. Zhao, X.-R. Liu, X. Wang, J. Hu, Y.-J. Cai, Q.-A. Peng, *Acta Chim. Slov.* **2021**, *68*, 804–810; **DOI:**10.17344/acsi.2021.6781
   (d) S. Han, Y. Wang, *Acta Chim. Slov.* **2021**, *68*, 961–969. **DOI:**10.17344/acsi.2021.6965
8. (a) M. Ahmed, M. Imran, M. Muddassar, R. Hussain, M.U. Khan, S. Ahmad, M.Y. Mehboob, S. Ashfaq, *J. Mol. Struct.* **2020**, *1220*, 128740; **DOI:**10.1016/j.molstruc.2020.128740
   (b) F. Naz, Kanwal, M. Latif, U. Salar, K.M. Khan, M. al-Rashida, I. Ali, B. Ali, M. Taha, S. Perveen, *Bioorg. Chem.* **2020**, *105*, 104365. **DOI:**10.1016/j.bioorg.2020.104365
9. (a) S. Hosny, G.A. Gouda, S.M. Abu-El-Wafa, *Appl. Organomet. Chem.* **2022**, e6627;
   (b) N. Biswas, S. Saha, B.K. Biswas, M. Chowdhury, A. Rahaman, V. Junghare, S. Mohapatra, S. Hazra, E. Zangrando, R.R. Choudhury, *J. Coord. Chem.* **2021**, *74*, 1482–1504; **DOI:**10.1080/00958972.2021.1913128
   (c) W.-G. Zhang, J.-H. Liang, *Acta Chim. Slov.* **2021**, *68*, 921–929; **DOI:**10.17344/acsi.2021.6902
   (d) C. Liu, *Acta Chim. Slov.* **2021**, *68*, 983–989; **DOI:**10.1515/dzph-2020-0068
   (e) Y. Yuan, X.-K. Lu, G.-Q. Zhou, X.-Y. Qiu, *Acta Chim. Slov.* **2021**, *68*, 1008–1015; **DOI:**10.17344/acsi.2021.7070
   (f) J.-L. Hou, H.-Y. Wu, C.-B. Sun, Y. Bi, W. Chen, *Acta Chim. Slov.* **2020**, *67*, 860–865. **DOI:**10.17344/acsi.2020.5824
10. Bruker, SMART and SAINT, Bruker AXS Inc., Madison, **2002**.
11. G. M. Sheldrick. SADABS, University of Göttingen, Germany, **1996**.
12. G. M. Sheldrick, *Acta Crystallogr.* **2015**, *C71*, 3-8.
13. W.-J. Mao, P.-C. Lv, L. Shi, H.-Q. Li, H.-L. Zhu, *Bioorg. Med. Chem.* **2009**, *17*, 7531–7536. **DOI:**10.1016/j.bmc.2009.09.018
14. (a) C. J. Matthews, K. Avery, Z. Xu, L.K. Thompson, L. Zhao, D. O. Miller, K. Biradha, K. Poirier, M.J. Zaworotko, C. Wilson, A. E. Goeta, J. A. K. Howard, *Inorg. Chem.* **1999**, *38*, 5266–5276; **DOI:**10.1021/ic990598f

(b) L. N. Dawe, T. S. M. Abedin, T. L. Kelly, L. K. Thompson, D. O. Miller, L. Zhao, C. Wilson, M. A. Leech, J. A. K. Howard. *J. Mater. Chem.* **2006**, *16*, 2645–2659. **DOI:**10.1039/B602595A

15. (a) R. Vafazadeh, R. Esteghamat-Panah, A.C. Willis, A.F. Hill, *Polyhedron* **2012**, *48*, 51–57; **DOI:**10.1016/j.poly.2012.08.057 (b) H. Hosseini-Monfared, E. Pousaneh, S. Sadighian, S.W. Ng, *Z. Anorg. Allg. Chem.* **2013**, *639*, 435–442. **DOI:**10.1002/zaac.201200395
16. (a) H.S. Jena, J. Subramanian, V. Manivannan, *Inorg. Chim. Acta* **2011**, *365*, 177–182. **DOI:**10.1016/j.ica.2010.09.007
17. (a) C. Liu, *Acta Chim. Slov.* **2022**, *69*, 157–166; **DOI:**10.17344/acsi.2022.7176 (b) H.-Y. Liu, X. Gan, J.-Y. Ding, Z.-T. Li, Q. Chen, *Acta Chim. Slov.* **2021**, *68*, 693–699. **DOI:**10.17344/acsi.2021.6716
18. (a) L.-W. Xue, X. Fu, G.-Q. Zhao, Q.-B. Liu, *Acta Chim. Slov.* **2021**, *68*, 17–24; **DOI:**10.17344/acsi.2020.5817 (b) F.-M. Wang, L.-J. Li, G.-W. Zang, T.-T. Deng, Z.-L. You, *Acta Chim. Slov.* **2020**, *67*, 1155–1162. **DOI:**10.17344/acsi.2020.6056
19. (a) S.-F. Yu, X.-Y. Qiu, S.-J. Liu, *Acta Chim. Slov.* **2020**, *67*, 1301–1308; **DOI:**10.17344/acsi.2020.6321 (b) G.-P. Cheng, L.-W. Xue, C.-X. Zhang, *Acta Chim. Slov.* **2017**, *64*, 261–265. **DOI:**10.17344/acsi.2016.3036
20. Y. Y. Luo, J. Q. Wang, B. T. Zhang, Y. X. Guan, T. Yang, X. Y. Li, L. Y. Xu, J. Wang, Z. L. You, *J. Coord. Chem.* **2020**, *73*, 1765–1777. **DOI:**10.1080/00958972.2020.1795645
21. M. M. Duan, Y. M. Li, L. Y. Xu, H. L. Yang, F.W. Luo, Y. X. Guan, B. T. Zhang, C. L. Jing, Z.L. You, *Inorg. Chem. Commun.* **2019**, *100*, 27–31. **DOI:**10.1016/j.inoche.2018.12.009

Povzetek

Sintetizirali smo tri enojedrne komplekse bakra(II) in niklja(II), $[Cu(L^1)(NCS)(CH_3OH)]$ (**1**), $[Cu(L^2)(NCS)]$ (**2**) in $[Ni(L^2)(N_3)]$ (**3**), kjer sta L^1 in L^2 monoanionski obliki Schiffovih baz *N*'-(piridin-2-ilmetilen)pikolinohidrazida (HL^1) in 4-metil-2-(((piridin-2-ilmetil)imino)metil)fenola (HL^2), ter jih okarakterizirali z elementno analizo, IR in UV-Vis spektroskopijo ter monokristalno rentgensko analizo. Atom Cu je v kompleksu **1** kvadratno piramidalno koordiniran s tremi N atomi liganda L in N atomom tiocianatnega liganda v ekvatorialnem položaju ter z O atomom metanola v apikalnem položaju. Atoma Cu in Ni sta v kompleksih **2** in **3** kvadratno planarno koordinirana s tremi donorskimi atomi ligandov Schiffove baze in terminalnimi N atomi tiocianatnih in azidnih ligandov. Kompleksa **1** in **2** zavirata ureazo stročnice *Canavalia ensiformis* z vrednostjo IC_{50} 0,33 ± 0,12 oziroma 0,39 ± 0,10 μmol L^{-1}. Za preučitev interakcij med kompleksi in encimom je bila izvedena študija molekularnega dockinga.